A Low-Complexity Carrier Phase and Frequency Offset Estimator with Adaptive Filter Length for Coherent Receivers

Adaickalavan Meiyappan, Pooi-Yuen Kam, Hoon Kim

Department of Electrical and Computer Engineering, National University of Singapore, 4 Engineering Drive 3, Singapore 117576, elekampy@nus.edu.sg

Abstract We present a low-complexity joint carrier phase and frequency offset estimator, with adaptive sample averaging length according to the modulation format, signal-to-noise ratio, and laser linewidth. No preset parameters are required. It also achieves complete frequency estimation range.

Introduction

Elastic optical networks with flexible modulation formats are seen as a way to improve the spectral efficiency over varying link conditions[1]. This has several key implications on digital carrier estimators (CEs) in coherent receivers. The CE should handle dynamic modulation formats, varying signal-to-noise ratio (SNR) due to varying link states, and yet be computationally simple for feasible implementation. Moreover, the laser linewidth may vary in a reconfigurable optical network. Hence, the CE should be adaptive to a varying laser linewidth $\Delta\nu$, in addition to estimating the frequency offset Δf. Here, $\Delta\nu$ is the total linewidth of the transmitter and local oscillator lasers, whereas Δf is the frequency difference between the two lasers.

The modulation format, SNR, and $\Delta\nu$ affects the optimal sample averaging filter length in prevalent fundamental phase estimators, namely, block Mth power[2,3] and blind phase search (BPS)[4] estimators. However, their averaging filter length cannot be adaptively adjusted; instead they require difficult numerical optimization and manual adjustment[2,4]. A poor choice of filter length directly affects the complexity besides degrading the bit-error rate (BER). An unnecessarily long filter length increases the required number of adders and multipliers for filtering. Next, consider prevalent frequency offset estimators, namely, fast Fourier transform based estimator (FFTbE)[5] and partitioning based differential frequency estimator (DiffFE)[6]. Both have limited frequency-offset-symbol-duration product, ΔfT, estimation range of $\pm 1/(2M)$ for M-ary phase-shift keying (MPSK) and $\pm 1/8$ for 16 quadrature amplitude modulation (QAM). Furthermore, FFTbE has an undesirably large $(N/2)log_2 N$ complex multiplications and $Nlog_2 N$ complex additions. N is the sample size for frequency estimation.

In this paper, by modifying our previous complex-weighted decision-aided maximum-likelihood (CW-DA-ML) CE[7], we present an adaptive complex-weighted decision-aided (CW-DA) CE. Our new CE is a two-tap joint phase and frequency estimator whose effective sample averaging length is adaptively adjusted depending on the modulation format, SNR, and $\Delta\nu$. A complete ΔfT estimation range of $\pm 1/2$ is attained. Thanks to the two-tap structure, drastic complexity simplification is achieved compared to other CEs.

Operating principle of adaptive CW-DA CE

Assuming perfect clock recovery, elimination of intersymbol interference, and ideal polarization demultiplexing by preceding digital signal processing blocks, the received signal at the CE is $r(k) = m(k)\exp\left[j\left(2\pi\Delta fTk + \theta(k)\right)\right] + n(k)$. Here, $m(k)$ is the kth data symbol, $\theta(k)$ is the laser phase noise modeled as a Wiener process[4], and $n(k)$ is additive white Gaussian noise (AWGN). In CW-DA-ML CE[7], a reference phasor (RP) $V(k+1)$ of the carrier at time $k+1$ was formed using a filter of length L as

$$V(k+1) = C(k)\sum_{l=k-L+1}^{k} w_{k+1-l}(k)\, r(l)\hat{m}^*(l) \quad (1)$$

where $C(k)$ is a normalizing factor, each w_l is a complex filter weight, and $\hat{m}^*(l)$ is the conjugate of the receiver's decision on the lth symbol. To avoid specifying an L, we replace RP $V(k+1)$ by a new RP $\bar{V}(k+1)$ formed recursively as

$$\bar{V}(k+1) = \bar{w}_1(k)\bar{V}(k) + \bar{w}_2(k)\, r(k)/\hat{m}(k). \quad (2)$$

No normalization factor is required in (2) as the filter input $r(k)/\hat{m}(k)$ is normalized. Our new CE is applicable to both MPSK and MQAM due to the decision-aided approach of (2). The phase of the complex filter weights $\bar{w}_1$ and $\bar{w}_2$ is designed to rotate the current $\bar{V}(k)$ and input $r(k)/\hat{m}(k)$ by $2\pi\Delta fT$ radian to track the angular frequency offset, since a frequency error offsets consecutive samples by $2\pi\Delta fT$. Magnitude of $\bar{w}_1$ and $\bar{w}_2$ is designed to control the effective sample averaging length by summing past samples in a decaying manner. The RP $\bar{V}(k)$ estimates the value $\exp[j(2\pi\Delta fTk + \theta(k))]$.

Filter weights are chosen automatically at each time k to minimize the cost function $J(k)$,

$$J(k) = \sum_{l=1}^{k} \left| \frac{r(l)}{\hat{m}(l)} - \bar{V}(l) \right|^2 . \quad (3)$$

Here, $|\cdot|$ denotes modulus. In (3), $\bar{V}(k)$ is forced to track the target $r(k)/\hat{m}(k)$. Using (2) to express $\bar{V}(l)$ in (3) and solving $\partial J(k)/\partial \bar{\boldsymbol{w}}^*(k) = 0$ for $\bar{\boldsymbol{w}}(k)$, where $\bar{\boldsymbol{w}}(k) = [\bar{w}_1(k)\ \ \bar{w}_2(k)]^T$, gives

$$\bar{\boldsymbol{w}}(k) = \boldsymbol{\Phi}^{-1}(k) \cdot \boldsymbol{z}(k), \qquad k \geq 1$$

$$\boldsymbol{\Phi}(k) = \sum_{l=1}^{k} \begin{bmatrix} |\bar{V}(l-1)|^2 & \bar{V}^*(l-1)x(l-1) \\ x^*(l-1)\bar{V}(l-1) & |x(l-1)|^2 \end{bmatrix}$$

$$\boldsymbol{z}(k) = \sum_{l=1}^{k} x(l) \begin{bmatrix} \bar{V}^*(l-1) \\ x^*(l-1) \end{bmatrix} \quad (4)$$

Here, $x(l) = r(l)/\hat{m}(l)$, while superscript T and $*$ denote transpose and conjugate, respectively. Use of decision symbol $\hat{m}(l)$ in (4) enables the filter weights, and thus the effective sample averaging length, to be adapted according to the format used. The weights are initialized to $\bar{w}_1(0) = 0$ and $\bar{w}_2(0) = 1$.

Inversion of the 2-by-2 matrix $\boldsymbol{\Phi}(k)$ is trivial, whereas the summations in $\boldsymbol{\Phi}(k)$ and $\boldsymbol{z}(k)$ can be computed as a running sum. Moreover, $\boldsymbol{\Phi}(k)$ is Hermitian, thus only the upper triangle needs to be computed and stored. Hence, we save on computation and memory resources.

Results and discussion

Automatic filter weight adaptation, averaged over 500 runs, in a single-polarization 28-Gbaud 16-QAM signal with ΔfT = 0.1 is shown in Fig. 1. Fig. 1(a) shows $|\bar{w}_1|$ increasing while $|\bar{w}_2|$ decreases to a steady state, starting from initial values of 0 and 1, respectively. The steady state value of $|\bar{w}_1|$ increases when SNR per bit, γ_b, is reduced from 12 dB to 9 dB, as averaging over larger sample size is beneficial in reducing the effect of increased AWGN. Note that larger $|\bar{w}_1|$ implies a slower decay rate and a longer effective sample averaging length. As linewidth $\Delta\nu$ increases from 200 kHz to 2 MHz, the steady state value of $|\bar{w}_1|$ decreases. Broader laser linewidth causes faster decorrelation of the phase noise $\theta(k)$ from $\theta(k-l)$. Hence, averaging over a smaller sample size gives better phase estimate at higher $\Delta\nu$. Regardless of SNR and $\Delta\nu$, the sum $|\bar{w}_1| + |\bar{w}_2|$ always converges to 1. Hence, past samples are summed in a decaying manner and magnitude of $\bar{V}(k)$ is forced to ~1. In Fig. 1(b), the phase of both filter weights converges quickly to the actual angular frequency offset value $2\pi\Delta fT$ = 0.628, regardless of the SNR and $\Delta\nu$. Since the

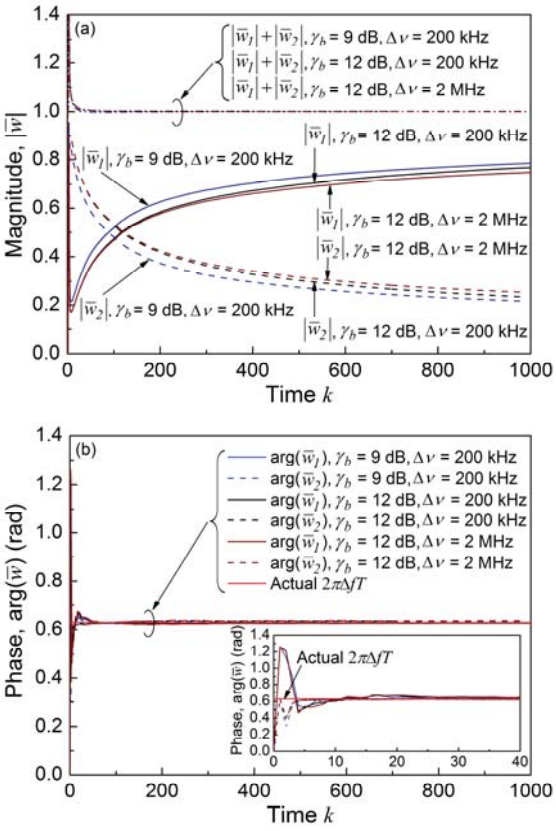

Fig. 1: Adaptation of the (a) magnitude of weights, $|\bar{w}|$, and (b) phase of weights, $arg(\bar{w})$. Inset shows enlarged time $0 \leq k \leq 40$.

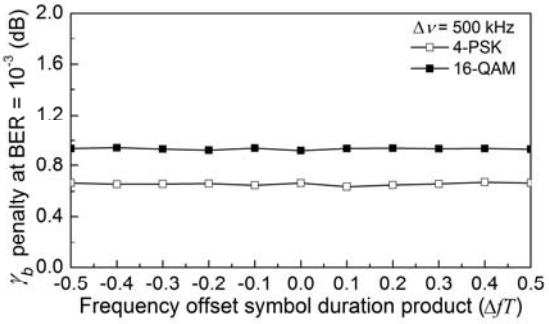

Fig. 2: Frequency offset estimation range.

current $\bar{V}(k)$ and input $r(k)/\hat{m}(k)$ have an angular frequency offset approximating $2\pi\Delta fTk$, they need to be rotated by an additional $2\pi\Delta fT$ radian to track the angular frequency offset of $2\pi\Delta fT(k+1)$ in the sample $r(k+1)$. Results of Fig. 1 show that the magnitude of the filter weights controls the effective sample averaging length depending on SNR and $\Delta\nu$, while the phase of the filter weights helps track the angular frequency offset.

Fig. 2 plots the γ_b penalty compared to ideal coherent detection versus ΔfT for adaptive CW-DA CE in 28-Gbaud 4-PSK and 16-QAM, with $\Delta\nu$ = 500 kHz. It demonstrates our new CE having a format-flexible, complete ΔfT

Tab. 1: Complexity comparison for 16-QAM

Estimator	Real adders	Real multipliers	Decision devices	Comparators	Table look-up	Buffer units
BPS	$(L+4)\beta$	6β	β	β	0	$L\beta$
	736	192	32	32	0	608
DiffFE-BPS	$4N-2+(L+4)\beta$	$7N+1+6\beta$	β	$2+\beta$	1	$L\beta$
	40734	70193	32	34	1	608
DiffFE-Mth	$4N+15-2/L$	$7N+25+5/L$	0	$2+(L+4)/2L$	$1+1/L$	0
	40014.9	70025.25	0	2.6	1.05	0
CW-DA-ML	$6L^2+8L+6$	$6L^2+14L+10$	0	0	0	L^2+6L+4
	966	1042	0	0	0	220
Adaptive CW-DA	34	43	0	0	0	12

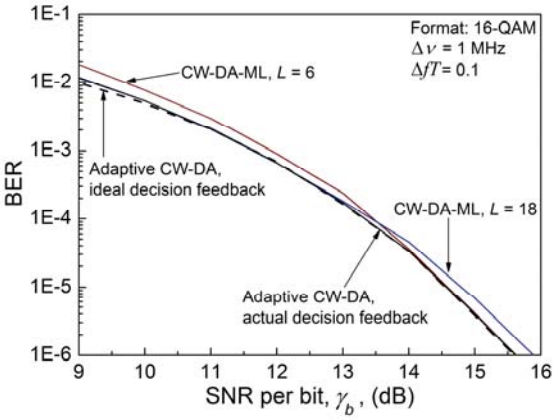

Fig. 3: BER performance at $\Delta\nu$ = 1 MHz, ΔfT = 0.1.

estimation range of $\pm 1/2$. Fig. 3 compares the BER of CW-DA-ML and adaptive CW-DA CE in 16-QAM at $\Delta\nu$ = 1 MHz, ΔfT = 0.1. The optimum filter length L of CW-DA-ML CE, yielding the best BER, is larger for low SNR and smaller for high SNR. Averaging over a longer window is necessary to reduce the dominant AWGN at low SNR, whereas a shorter averaging window is necessary for the quickly decorrelating phase noise which is dominant at high SNR. Search for the optimum L at each SNR and $\Delta\nu$ requires exhaustive simulations. On the other hand, adaptive CW-DA CE yields the lower BER at all times by adaptively adjusting its effective sample averaging length according to the SNR and $\Delta\nu$. Performance degradation of adaptive CW-DA CE with actual, compared to ideal, decision feedback is negligible for BER values below 10^{-3}. Differential encoding was used to prevent cycle slips in Fig. 2 and Fig. 3.

The total hardware complexity required to produce a carrier phase and frequency estimate is listed in Tab. 1 for 16-QAM. The $1/L$ fraction arises due to resource sharing in block Mth power scheme. DiffFE-BPS[4,6] and DiffFE-Mth[3,6], are combinations of the frequency and phase estimators. Complexity of BPS alone to produce a phase estimate is included in Tab. 1 for reference, where β is the number of test phases. Actual numbers are also given by substituting for BPS (L = 19, β = 32)[4], DiffFE-BPS (N = 10^4, L = 19, β = 32)[4,6], DiffFE-Mth (N = 10^4, L = 20)[3,6], and CW-DA-ML (L = 12). Although estimating both phase and frequency, our new CE requires 4.5 times less real multipliers than the pure phase estimator BPS. BPS based estimators have a complexity which is filter-length dependent and increases with modulation order due to the increasing β requirement[4]. In contrast, our new CE has a fixed format-transparent complexity. Our new CE consumes the least adders, multipliers, and buffer units among the CEs in Tab. 1, yet not requiring any intermediate decision devices, comparators, or table look-ups. A multiplier reduction of >24 times is achieved compared to CW-DA-ML CE.

Conclusion

A flexible, low-complexity, joint carrier phase and frequency estimator is presented. The optimal sample averaging length is automatically adapted according to the modulation format, SNR, and laser linewidth present, without any *a priori* system statistics. Hence, the estimator is suitable for future elastic and reconfigurable optical networks. Our new estimator also has full frequency offset estimation range.

References

[1] O. Grestel et al., IEEE Commun. Mag., **50**, s12-s20 (2012).
[2] M. Seimetz, Proc. OFC, OTuM2 (2008).
[3] I. Fatadin et al., IEEE Photon. Technol. Lett., **22**, 631-633 (2010).
[4] T. Pfau et al., J. Lightw. Technol., **27**, 989-999 (2009).
[5] M. Selmi et al., Proc. ECOC, P3.08 (2009).
[6] I. Fatadin et al., IEEE Photon. Technol. Lett., **23**, 1246-1248 (2011).
[7] A. Meiyappan et al., Proc. OFC, OTu3I.4 (2013).